J Therm Anal Calorim (2012) 109:481–486
DOI 10.1007/s10973-011-1301-7

# Phase behaviour of tri-*n*-butylmethylammonium chloride hydrates in the presence of carbon dioxide

**Nadia Mayoufi · Didier Dalmazzone ·
Walter Fürst · Leila Elghoul · Adel Seguatni ·
Anthony Delahaye · Laurence Fournaison**

Received: 9 July 2010 / Accepted: 4 January 2011 / Published online: 5 February 2011

**Abstract** The phase behaviour of the system water–tri-*n*-butylmethylammonium chloride (TBMAC)–$CO_2$ was investigated by pressure-controlled differential scanning calorimetry in the range 0–10 mol% TBMAC in water and at $CO_2$ pressures ranging from 0 to 1.5 MPa. In the absence of $CO_2$, an incongruent melting hydrate, which estimated composition corresponds to TBMAC·$30H_2O$, crystallizes at temperatures below −13.6 °C and forms with ice a peritectic phase at approximately 3.9 mol% TBMAC. In the presence of $CO_2$ at pressures as low as 0.5 MPa, curves evidenced the presence of an additional phase exhibiting congruent melting at temperatures that are strongly pressure dependent and significantly higher than those of hydrates obtained without $CO_2$. This new phase, whose enthalpy of dissociation and $CO_2$ content increase slightly with $CO_2$ pressure, was identified as a mixed semi-clathrate hydrate of TBMAC and $CO_2$ of general formula: $(\mathrm{TBMAC} + x\mathrm{CO_2})\cdot 30\mathrm{H_2O}$.

**Keywords** Semi-clathrate hydrate · $CO_2$ · Tetra-alkyl ammonium salt · Equilibrium · Dissociation enthalpy

---

N. Mayoufi · D. Dalmazzone (✉) · W. Fürst · L. Elghoul · A. Seguatni
ENSTA ParisTech, 32 Boulevard Victor, 75739 Paris Cedex 15, France
e-mail: didier.dalmazzone@ensta.fr

A. Delahaye · L. Fournaison
CEMAGREF, Refrigeration Processing Research Unit, 92163 Antony, France

## Introduction

Clathrate hydrates are crystalline structures in which water molecules associated via hydrogen bonds form cavities of various shapes. Small hydrophobic molecules, mostly light hydrocarbons (C1–C8), acid gases ($CO_2$, $H_2S$) or cyclic ethers (tetrahydrofurane), may be inserted in these cavities and, under proper pressure and temperature conditions, stabilize the hydrate by Van der Waals interactions with the aqueous network. Semi-clathrate hydrates are formed from water and various organic salts associating a tetra-alkyl ammonium or phosphonium cation combined with a variety of anions ($F^-$, $Cl^-$, $Br^-$, $NO_3^-$, $OH^-$…) [1]. In these structures, the alkyl groups are trapped in the cavities formed by water, in a hydrophobic interaction scheme similar to what is encountered in clathrate hydrates. In addition, the anion is inserted into the water network, which it stabilizes via hydrophilic interactions. Such structures have been extensively studied by Dyadin et al. [1, 2].

Hydrates of tetra-*n*-butylammonium salts, especially the bromide (TBAB), are generally considered as promising materials for various innovating processes. Because of its high latent heat and suitable temperature of melting [3], TBAB semi-clathrate hydrate has been proposed as a phase change material (PCM) for cold transport in a novel refrigeration process [4].

Some semi-clathrate hydrates have long been known to have the capacity of hosting gases in free cavities present in their structures [5]. TBAB and TBAF (fluoride) form double hydrates with $CO_2$, $CH_4$ or $H_2$. $CO_2$ + TBAB double hydrate was recently proposed as a more efficient PCM than single TBAB hydrate, to be used in secondary refrigeration [6]. One of the advantages of semi-clathrates is that their dissociation temperature may be varied from less than 0 to more than 30 °C [1] depending on the nature of the additive. Inserting gas molecules to form mixed hydrates generally stabilizes the structure, increasing both the temperature and the enthalpy of dissociation [7]. If such mixed hydrates could be formed with several additives, they would provide a variety of efficient PCMs for thermal energy storage, with temperatures of transition adapted to various ranges of applications. Other potentialities, including gas storage and gas separation could also be developed.

We present a study undertaken on a hydrate formed by tri-*n*-butylmethylammonium chloride (TBMAC) alone and in the presence of carbon dioxide. Pressure-controlled differential scanning calorimetry (HP-DSC) has been validated as a convenient technique to study gas hydrates [7–13]. It provides precious information on both thermodynamic stability and latent heat of phase change. In this study, this technique was used to investigate the $CO_2$ pressure effect on the phase behaviour and the enthalpy changes in the system $CO_2 + TBMAC + H_2O$. In addition, IR spectrometry experiments were performed for the determination of the hydrate composition.

## Experimental

### Materials

Analytical grade TBMAC ([56375-79-2], 98 wt%) was purchased from Fluka and used with no further purification. Freshly distilled water was carefully degassed before preparing a total of 18 solutions. Their concentrations, ranging from 0 (pure water) to 60% TBMAC in mass (0–10% in mol), are summarized in Table 1. N45 grade $CO_2$ (99.995 vol%) was purchased from Air Liquide.

**Table 1** Concentrations of the TBMAC solutions studied

| Wt% | Mol% | Wt% | Mol% | Wt% | Mol% |
|---|---|---|---|---|---|
| 0.0 | 0.00 | 15.0 | 1.30 | 38.0 | 4.39 |
| 2.5 | 0.19 | 17.5 | 1.56 | 40.0 | 4.75 |
| 5.0 | 0.39 | 20.0 | 1.84 | 45.0 | 5.77 |
| 7.5 | 0.60 | 25.0 | 2.43 | 50.0 | 6.96 |
| 10.0 | 0.82 | 32.0 | 3.40 | 55.0 | 8.38 |
| 12.5 | 1.06 | 35.0 | 3.87 | 60.0 | 10.10 |

### HP-DSC experimental setup and protocol

The experimental setup has been described previously [7, 12, 13]. It is based on a high sensitivity DSC (micro DSC VII from Setaram, France). As illustrated in Fig. 1, the DSC device is equipped with two pressure-controlled Hastelloy cells. Sample cell (E) was charged with the sample solution, whilst the reference cell (R) was left empty. The feed gas cylinder was connected to the sample cell via a simple stage pressure regulator that allowed the working pressure to be adjusted from ambient to 3 MPa. Pressure was measured by a Druck gauge (0–3 MPa) with a resolution of 0.001 MPa. The temperature and enthalpy calibration of the DSC in the range −40–30 °C was realized using the melting of high purity mercury and gallium samples. Ice melting experiments were performed to control the accuracy of measured enthalpy, which was found to be better than 1%, and temperature of phase change, which was better than 0.2 °C with a repeatability of 0.05 °C.

After charging the sample cell with 50–60 μL of solution and carefully weighing with a $10^{-5}$ g precision analytical balance, the cell was inserted into the furnace and connected to the gas feed line.

For each sample, a blank experiment was first performed at ambient pressure with no $CO_2$ added. Then, the sample cell was purged with $CO_2$ to evacuate the air and $CO_2$ pressure was set to the desired value and kept constant during each determination. The same temperature programme was repeated at increasing $CO_2$ pressures, from 0.5 to 1.5 MPa. It consisted in a cooling sequence down to −30 °C at a rate of 2 °C $min^{-1}$, an isotherm at −30 °C for 20 min to allow sample crystallization and a warming sequence up to 25 °C at 0.5 °C $min^{-1}$ to melt the solids. The heat flow (mW) was recorded either in cooling or warming sequences. Warming heat flow curves were used for the determination of congruent and incongruent melting temperatures according to the protocol that has been described in details [12, 13].

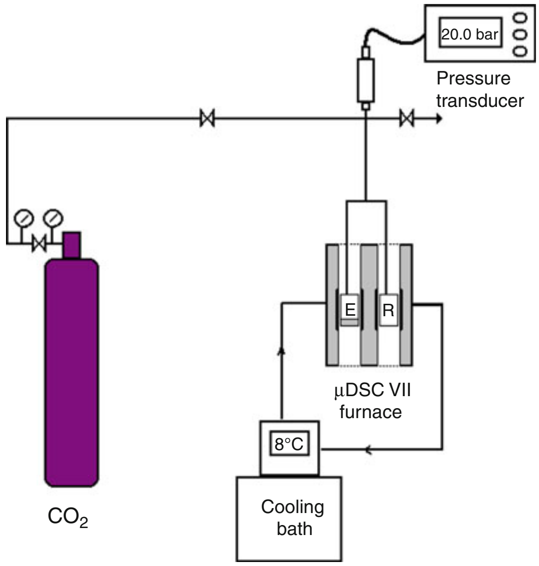

**Fig. 1** HP-DSC device. *E* sample cell. *R* reference cell

### Phase analysis

Ambient pressure reactor experiments were performed in a 100 cm$^3$ Pyrex jacketed reactor equipped with a valve at its bottom end to allow the liquid phase to be evacuated after partial crystallization (Fig. 2). The reactor was flushed by inert gas ($N_2$) flow to avoid ambient moisture condensation and to help evacuating the liquid.

After preparing the hydrate in the reactor, the crystals were warmed up at room temperature and the resulting solution was analysed by IR spectrometry (Tensor 27 from Brucker equipped with an ATR crystal) to determine its TBMAC concentration. Figure 3 presents IR spectra obtained with solutions of various concentrations. The band at 2850–2900 cm$^{-1}$ is situated in the spectral region corresponding to C–H bond vibration modes and is therefore specific of the alkyl groups bonded to the ammonium ion. Its intensity increases regularly with TBMAC concentration, thus providing the calibration curve presented in Fig. 4.

## Results and discussion

### TBMAC + $H_2O$ system

Because no data could be found in the literature on the phase behaviour in the TBMAC + water system, we studied the melting of the solid phases formed in solutions of variable concentrations reported in Table 1. The curves obtained upon warming at 0.5 °C min$^{-1}$ after crystallizing the samples at −30 °C are reported in Fig. 5 for 0.19–3.40 mol% (2.5–32 wt%) solutions and in Fig. 6 for 3.87–10.10 mol% (35–60 wt%) solutions. Below 3.87 mol%, the curves show two peaks. The first one appears as a constant temperature melting peak, at −13.6 ± 0.1 °C. The second one is a progressive melting peak which temperature decreases with increasing TBMAC concentration.

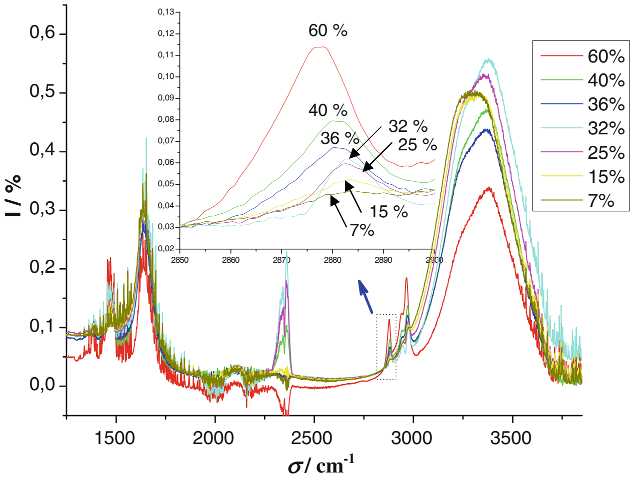

**Fig. 3** IR spectra of TBMAC solutions of various concentrations (in wt%)

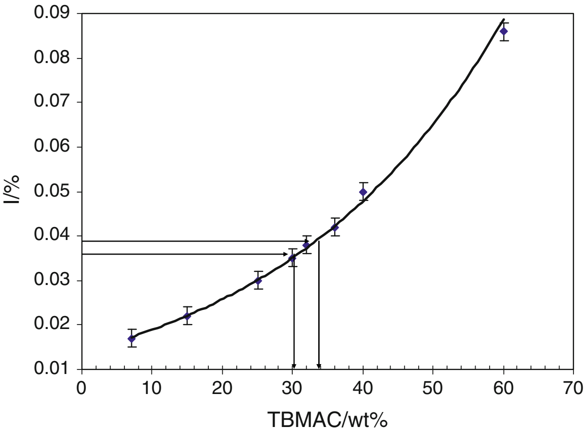

**Fig. 4** Calibration curve giving the intensity of the IR band at 2850–2900 cm$^{-1}$ as a function of TBMAC concentration

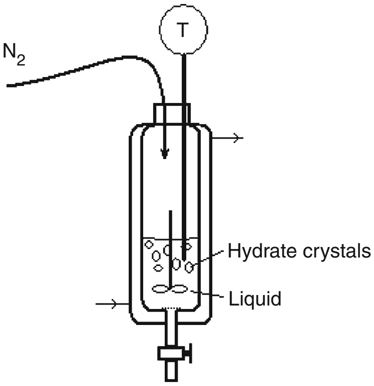

**Fig. 2** Reactor for TBMAC hydrate synthesis under neutral atmosphere at ambient pressure

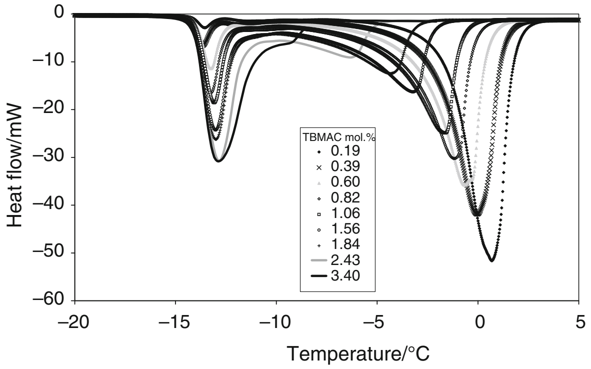

**Fig. 5** Heat flow curves obtained with the TBMAC solutions of concentrations 0.19–3.40 mol%

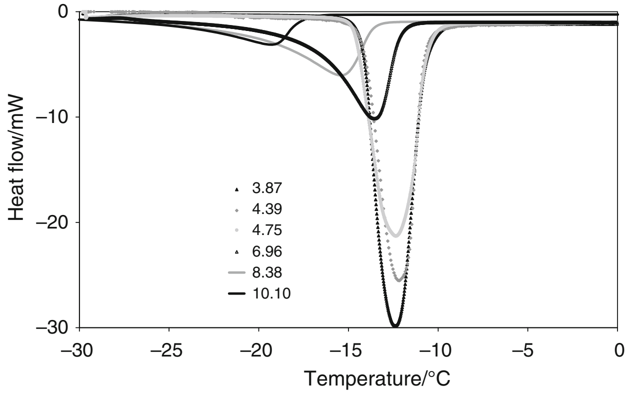

**Fig. 6** Heat flow curves obtained with the TBMAC solutions of concentrations 3.87–10.10 mol%

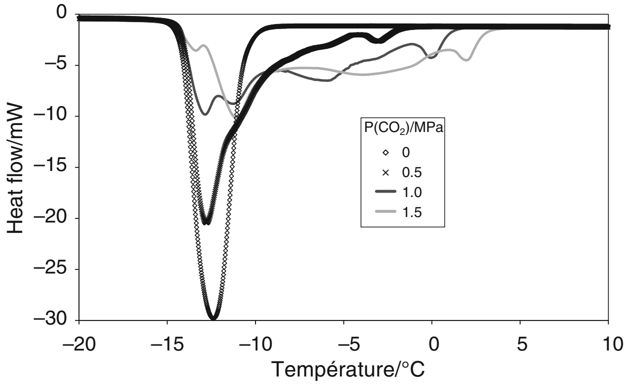

**Fig. 8** Heat flow curves obtained with a 3.87 mol% TBMAC solution at various $CO_2$ pressures

Figure 7 represents the measured melting temperatures versus TBMAC concentration. The constant melting temperatures form a horizontal line from 0 to 3.87 mol% TBMAC. The ending temperatures of progressive melting peaks form two liquidus branches that join at point P. These results suggest the existence of an incongruent melting compound TBMAC·$n$H$_2$O, forming a peritectic phase with ice. The peritectic point P corresponds to the intersection of ice and hydrate melting curves. In agreement with the Gibbs rule, this four phase point (hydrate + ice + liquid + vapour) is a non variant point which coordinates can be evaluated: 3.9 TBMAC mol% approximately in composition and −13.6 °C for the melting temperature.

In order to determine the hydration number $n$, we prepared the hydrate by maintaining a TBMAC solution of concentration greater than 4 mol% in a reactor (Fig. 2) at −20 °C. These conditions are within the (hydrate + liquid) region of the phase diagram of Fig. 7, thus leading to the formation of a diphasic mixture. After removing the liquid phase, the hydrate crystals were carefully dried under slow nitrogen flushing and then warmed up at room temperature for IR analysis of the resulting solution. Several experiments were repeated, resulting in a TBMAC content comprised between 3.1 and 3.3 mol%. This corresponds to a hydration number comprised between 29.3 and 31.3, and we thus assume the formula TBMAC·30H$_2$O for the TBMAC hydrate.

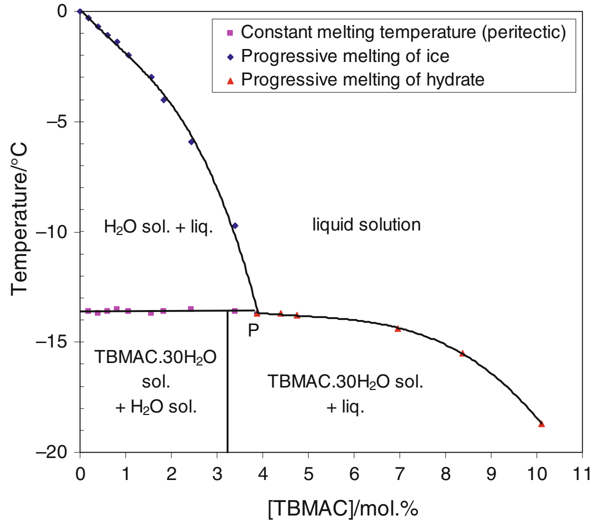

**Fig. 7** TBMAC + H$_2$O binary phase diagram

## TBMAC + $CO_2$ + $H_2O$ system

### *Phase behaviour*

Figure 8 compares the heat flow curves obtained with one of the TBMAC solutions (3.87 mol%), alone and in the presence of $CO_2$ at increasing pressures. This composition is very close to the non variant peritectic point of the TBMAC–H$_2$O diagram (Fig. 7) and the corresponding signal is an unique, constant temperature melting peak. As $CO_2$ pressure is increased, this peak tends to disappear and

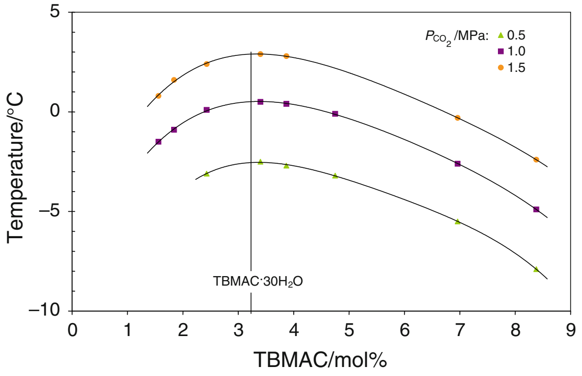

**Fig. 9** Isobar phase boundaries in the TBMAC + H$_2$O + CO$_2$ ternary at three different CO$_2$ pressures: 0.5, 1.0 and 1.5 MPa. *Points* experimental results; *lines* polynomial representation; *vertical line* 3.23 mol% corresponding to TBMAC·30H$_2$O hydrate

**Table 2** Temperatures and enthalpies of dissociation and approximate composition of the mixed TBMAC + $CO_2$ semi-clathrate hydrate at various $CO_2$ pressures

| $P_{CO_2}$/MPa | $T_{diss}$/°C | $\Delta H_{diss}$/J $g^{-1}$ | $\Delta H_{diss}$/J $mol^{-1}_{H_2O}$ | Estimated formula |
|---|---|---|---|---|
| 0 | −13.6 | 250.2 | 4504 | TBMAC·$30H_2O$ |
| 0.5 | −3.9 | 217.5 | 5592 | (TBMAC + 1.5 $CO_2$)·$30H_2O$ |
| 1.0 | 0.5 | 225.7 | 5804 | (TBMAC + 1.6 $CO_2$)·$30H_2O$ |
| 1.5 | 2.1 | 257.2 | 6614 | (TBMAC + 1.8 $CO_2$)·$30H_2O$ |

to be replaced by several additional signals, which demonstrate the presence of new solids. The last peak appears 10–15 °C higher than the dissociation of TBMAC hydrate obtained without $CO_2$, thus emphasizing the high stabilisation effect of the gas. Intermediate peaks denote the melting of metastable phases, which are very often formed in DSC experiments conducted on gas–liquid–solid systems due to the lack of stirring. Only the most stable phase, which melts at the highest temperature, is thermodynamically relevant.

The same experiment was repeated with various TBMAC solutions at $CO_2$ pressures of 0.5, 1 and 1.5 MPa. Dissociation temperatures corresponding to the last peak are gathered in Fig. 9. Solid curves were obtained by adjusting a third order polynomial to each set of points. The phase boundaries evidence a congruent melting compound marked by the vertical line, having a TBMAC/$H_2O$ molar ratio very close to that of the incongruent melting TBMAC hydrate.

The effect of pressure on the phase behaviour of semi-clathrate hydrates has been described by Dyadin [1]. It is common that some phases that melt incongruently at ambient conditions become stabilized and thus exhibit congruent melting at pressures of a few tens of MPa. In the case presented here, however, the very low gas pressure used would not be sufficient to stabilize the TBMAC hydrate to such extent. We therefore invoke the insertion of $CO_2$ into available cavities of the semi-clathrate structure to explain the stabilisation, similarly to what is observed with many other comparable hydrates [5, 7].

### *Dissociation enthalpy and $CO_2$ content*

In order to measure the enthalpy of dissociation of the hydrate, full conversion of the solution sample must be achieved and any trace of the metastable phases must be eliminated. We used a multi-cycle temperature programme as described in details in [13] to achieve the formation of 100% of stable (TBMAC + $x$$CO_2$)·$30H_2O$ mixed hydrate. 3.4 mol% TBMAC solution samples were used for enthalpy determinations, which is very close to the supposed composition of the congruent melting hydrate.

An estimate of the gas content of the mixed hydrate can be obtained from the enthalpy measurements in combination with the enthalpy deduced from equilibrium points using Clausius–Clapeyron relation [7, 13]:

$$\frac{\partial \ln P}{\partial(1/T)} = -\frac{\Delta H}{ZR}.$$

The dissociation enthalpy $\Delta H$ is expressed here on a J $mol^{-1}_{CO_2}$ basis, whilst measurements of the same enthalpy performed by DSC can be expressed on a J $mol^{-1}_{H_2O}$ basis, thus providing an evaluation of the $CO_2$ to $H_2O$ molar ratio in the hydrate composition. The limits and uncertainty of this method have been discussed in [7]. Using this relation with the ($P$, $T$) points obtained for the 3.4 mol% TBMAC solution gave an enthalpy of dissociation $\Delta H = 109811$ J $mol^{-1}_{CO_2}$. The results obtained for the enthalpy measurements by DSC at 0.5, 1 and 1.5 MPa $CO_2$ pressures reported in Table 2 are expressed in J $g^{-1}$ of solution sample and converted to J $mol^{-1}$ of water. The resulting estimated compositions of the hydrate are also presented in Table 2.

## Conclusions

The phase diagram of the TBMAC–water binary system was obtained from DSC dissociation temperature measurements. It exhibits a non congruent melting hydrate that forms at temperatures below −13.6 °C and which composition could be estimated to TBMAC·$30H_2O$ by IR spectrometry.

The hydrate's melting temperature is strongly increased by applying $CO_2$ pressure between 0.5 and 1.5 MPa and, moreover, melting becomes congruent. The stabilisation of the hydrate structure due to the presence of $CO_2$ is confirmed by the measurement of its enthalpy of dissociation, which slightly increases with $CO_2$ pressure from 0 to 1.5 MPa. This leads to the conclusion that the hydrate is capable of entrapping gas molecules into available cavities, on the same scheme as many other semi-clathrate discovered previously. The gas uptake as a function of pressure was estimated, leading to a global formula of the mixed hydrate: (TBMAC + $x$$CO_2$)·$30H_2O$, where $x$ varies from 1.5 to 1.8 when $P_{CO_2}$ is increased from 0.5 to 1.5 MPa.

The new mixed hydrate exhibits a dissociation enthalpy close to that of ice melting and a range of melting temperatures comprised between −4 and +2 °C at moderate pressure. It may thus be considered as a potential PCM having properties well suited for cold storage and transportation.

**Acknowledgements** The ADEME is acknowledged for financial support (contract 05 74 C 0013).

## References

1. Dyadin YuA, Udachin KA. Clathrate formation in water-peralkylonium salts systems. J Incl Phenom. 1984;2:61–72.
2. Aladko LS, Dyadin YuA, Rodionova TV, Terekhova IS. Clathrate hydrates of tetrabutylammonium and tetraisoamylammonium halides. J Struct Chem. 2002;43(6):990–4.
3. Oyama H, Shimada W, Ebinuma T, Kamata Y, Takeya S, Uchida T, Nagao J, Narita H. Phase diagram, latent heat, and specific heat of TBAB semiclathrate hydrate crystals. Fluid Phase Equilib. 2005;234(1–2):131–5.
4. Tanasawa I, Takao S. Clathrate hydrate slurry of tetra-*n*-butylammonium bromide as a cold-storage material. In: 4th International Conference on Gas Hydrates, vol 2, Yokohama, Japan, p. 963–967, 19 to 23 May 2002.
5. Arjmandi M, Chapoy A, Tohidi B. Equilibrium data of hydrogen, methane, nitrogen, carbon dioxide and natural gas in semi-clathrate hydrates of tetrabutylammonium bromide. J Chem Eng Data. 2007;52(6):2153–8.
6. Lin W, Delahaye A, Fournaison L. Phase equilibrium and dissociation enthalpy for semi-clathrate hydrate of $CO_2$ plus TBAB. Fluid Phase Equilib. 2008;264(1–2):220–7.
7. Mayoufi N, Dalmazzone D, Fürst W, Delahaye A, Fournaison L. $CO_2$ enclathration in hydrates of peralkyl-(ammonium / phosphonium) salts: Stability conditions and dissociation enthalpies. J Chem Eng Data. 2010;55(3):1271–5. doi:10.1021/je9006212.
8. Dalmazzone D, Dalmazzone C, Herzhaft B. Differential scanning calorimetry: a new technique to characterize hydrate formation in drilling muds. SPE J. 2002;June:196–202.
9. Dalmazzone D, Kharrat M, Lachet V, Fouconnier B, Clausse D. DSC and PVT measurements of methane and trichlorofluoromethane hydrate dissociation equilibria in highly concentrated calcium chloride solutions and water-in-oil emulsions. J Therm Anal Calorim. 2002;70:493–505.
10. Kharrat M, Dalmazzone D. Experimental determination of stability conditions of methane hydrate in aqueous calcium chloride solutions using high pressure differential scanning calorimetry. J Chem Thermodyn. 2003;35:1489–505.
11. Dalmazzone D, Clausse D, Dalmazzone C, Herzhaft B. The stability of methane hydrates in highly concentrated electrolyte solutions by differential scanning calorimetry and theoretical computation. Am Mineral. 2004;89(8–9):1183–91.
12. Delahaye A, Fournaison L, Marinhas S, Chatti I, Dalmazzone D, Fürst W, Petitet J-P. Effect of THF on equilibrium pressure and dissociation enthalpy of $CO_2$ hydrates applied to secondary refrigeration. Ind Eng Chem Res. 2006;45:391–7.
13. Martinez MC, Dalmazzone D, Fürst W, Delahaye A, Fournaison L. Thermodynamic properties of THF + $CO_2$ hydrates in relation with refrigeration applications. AIChE J. 2008;54(4):1088–95.